Effects of Sulfuric Acid Concentration and Alloying Elements on the Corrosion Resistance of Cu-bearing low Alloy Steels

Ki Tae Kim and Young Sik Kim[†]

Materials Research Center for Clean and Energy Technology, School of Materials Science and Engineering, Andong National University, 1375 Gyeongdong-ro, Andong, Gyeongbuk, 36729, Korea

During the process of sulfur dioxide removal, flue gas desulfurization equipment provides a serious internal corrosion environment in creating sulfuric acid dew point corrosion. Therefore, the utilities must use the excellent corrosion resistance of steel desulfurization facilities in the atmosphere. Until now, the trend in developing anti-sulfuric acid steels was essentially the addition of Cu, in order to improve the corrosion resistance. The experimental alloy used in this study is Fe-0.03C-1.0Mn‒0.3Si-0.15Ni-0.31Cu alloys to which Ru, Zn and Ta were added. In order to investigate the effect of H_2SO_4 concentration and the alloying elements, chemical and electrochemical corrosion tests were performed. In a low concentration of H_2SO_4 solution, the major factor affecting the corrosion rate of low alloy steels was the exchange current density for H^+/H_2 reaction, while in a high concentration of H_2SO_4 solution, the major factors were the thin and dense passive film and resulting passivation behavior. The alloying elements reducing the exchange current density in low concentration of H_2SO_4, and the alloying elements decreasing the passive current density in high concentration of H_2SO_4, together play an important role in determining the corrosion rate of Cu-bearing low alloy steels in a wide range of H_2SO_4 solution.

Keywords: Cu-bearing low alloy steel, Sulfuric acid, Exchange current density, Passivation

1. Introduction

Fossil-fired power plants combust coal, oil, and gas, generate electricity using thermal energy from the combustion. When the coal, oil, and gas combust, the produced flue gas contains SO_x and NO_x, which induce acid rain of pH < 4.5. This acid rain may induce general corrosion or localized corrosion of the construction or steel structure. Therefore, to minimize the harmful exhaust gas, flue gas desulfurization (FGD) facility shall be installed and operated in every fossil-fired power plant.

The FGD facility is a system to eliminate sulfur dioxide from the flue gas formed when the fossil fuels are combusted. The exhaust acceptance criteria of dioxin, which is hazardous to human, are strictly limited, and thus the operating temperature of the FGD facility decreased, the sulfuric acid is then concentrated on the inside metal surface of FGD facility, and finally, dew point corrosion occurs. Therefore, corrosion resistant materials should be used for FGD facility [1-4].

Low alloy steel, one of the alloys used in the FGD

facility, has been developed to enhance the corrosion resistance. The recent report of Park *et al.* showed the beneficial effects of Cu, Mo and W additions in 10% H_2SO_4 solution [5], and others have reported the improvement of corrosion resistance to the sulfuric acid by Cu addition [6-15]. The solubility of 0.35% Cu at room temperature in ferrite phase was reported [16-17]. If Cu addition exceeds the solubility limit, fine precipitates can be formed and affect the corrosion properties; and when its content exceeds 0.5%, copper may be segregated on the surface of the steel at high temperature, because of the lower oxidation rate of copper than iron; and thus during hot working, the segregated copper penetrates into the inside of the steel and then red shortness may be induced [5]. Therefore, the content of copper should be controlled in an appropriate range.

The mechanism of improving the corrosion resistance of low alloy steel in sulfuric and acid-chloride media is based on suppressing anodic dissolution by re-depositing copper compounds on the steel surface immersed in corrosive condition [10]. Iron in the steel in acidic media selectively dissolves and copper in the matrix is also detached. The detached copper is dissolved into the sol-

---

[†] Corresponding author: yikim@anu.ac.kr

Table 1 Chemical composition of the experimental alloys (wt%)

Alloys	C	Mn	P	S	Si	Al	Cu	Ni	Ru	Zn	Ta	Fe
AH-1	0.03	0.95	0.023	0.004	0.3	0.049	0.31	0.36	-	-	-	Bal.
AH-2	0.01	0.97	0.025	0.004	0.3	0.055	0.32	0.16	0.11	-	-	Bal.
AH-3	0.03	1.0	0.025	0.004	0.3	0.097	0.31	0.15	-	0.006	-	Bal.
AH-4	0.01	1.0	0.026	0.004	0.3	0.057	0.31	0.15	-	-	0.12	Bal.

ution by dissolved oxygen and then presents as Cu^{2+} ion. According to the E-pH diagram, since the reduction potential of copper is more noble than the reduction potential of hydrogen, the enriched layer of copper formed on the surface, in order to use the electron evolved during the dissolution of iron and then the corrosion resistance of the copper containing low alloy steel in sulfuric acid solutions can be enhanced [5,10].

Besides Cu addition, several researchers have reported the effects of Mn, Co, W, Mo, Ti, and Nb [18-22]; but among these elements, copper is one of the essential alloying elements, because of its powerful effect in sulfuric acid solutions.

In the case of Sb addition, Sb oxide is formed on the metallic surface in sulfuric acid solutions, and to protect the matrix; Sb_2O_3 forms mainly to protect the inside, and some parts of Sb_2O_3 oxidize to Sb_2O_5 at the outer surface to protect the matrix [23,24]. When Sb and Cu are co-added, the formation and stabilization of a copper-enriched layer is facilitated by the formation of copper ion complex, but also its corrosion resistance can be improved by the formation of the protective Sb oxide on the surface [5]. However, Sb compounds are classified as grade 2B of carcinogenicity by the International Agency for Research on Cancer (IARC) and therefore Sb addition should be substituted by the others [25,26]. Thus, in this work, the literature for the chemical composition of commercial products, E-pH diagram, Cu binary phase diagram, exchange current density of H^+/H_2 reaction, equilibrium potential, etc. were surveyed [27-33], and we chose 3 elements of Ru, Zn, and Ta. When Ru is added to stainless steels, it increases the corrosion potential and passivates the surface. When Ru is added to high chromium super alloys, the corrosion resistance can be enhanced by the formation of an oxide layer [30,31]. Zn decreases the equilibrium potential and exchange current density of the H^+/H_2 reaction, and when Zn is added to low alloy steel, corrosion resistance is improved by the formation of a barrier layer [32,33]. Tantalum forms the oxide [29]. This work focused on the effect of Ru, Zn, and Ta addition

on the corrosion resistance of low alloy steels in sulfuric acid solution. In addition, we controlled the concentration of sulfuric acid, and through chemical and electrochemical experiments, elucidated the effect of the concentration of sulfuric acid on the corrosion behavior of Cu-bearing low alloy steels.

2. Material and methods

2.1 Alloy design and manufacturing

The low alloy steels evaluated in this study were prepared from high purity grade of Fe, C, Mn, Cu, and Ni. After melting and stabilization at 1,700 ^{o}C in a high medium frequency vacuum induction furnace, Ru, Zn, or Ta was added and finally melted for each specimen. Only solid sections of the cast ingots (150 mm × 150 mm × 300T mm) were taken to prepare the specimens. The sections were first soaked for 120 min., and hot-rolled to 3 mm at 1,200 ^{o}C. The hot-rolled specimens were annealed at 820 ^{o}C for 30 min. and, air-cooled. A small section was cut from each procedure and was used for chemical analysis. Table 1 presents the chemical composition of the experimental alloys.

2.2 Microstructure analysis

The specimen was cut to a size of 20 mm × 20 mm × 3 mm, and then ground with #2000 SiC paper, and polished with 3 μm diamond paste. Finally, the specimen was cleaned with ethyl alcohol, using an ultrasonic cleaner. The microstructure was observed by optical microscopy (AXIOTECH 100HD, ZEISS) and SEM-EDS (VEGA II LMU, Tescan), after etching by 3 % Nital solution. Also, an Electron Probe Micro Analyzer (EPMA-1600 15 KV) was used to identify the elemental distribution of the surface and the cross-section.

2.3 Sulfuric acid corrosion test

A corrosion cell of 1 L capacity of glass in which a water condenser was installed was used. The alloys were cut into 1.5 cm x 2 cm blocks, and ground to #120 grit
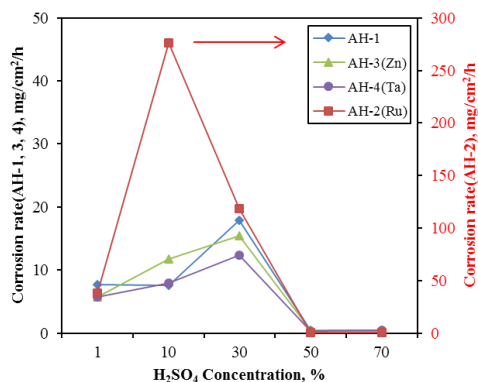
Fig. 1 Effect of sulfuric acid concentration on the corrosion rate of the experimental alloys (40 oC, 3 h immersion test).

of SiC paper. Test solutions were (1, 10, 30, 50, and 70) vol% H_2SO_4 and the immersion time was 3h. After the test and cleaning, the corrosion rate was calculated as the unit of $mg/cm^2/h$.

2.4 Anodic polarization test

Specimens were cut to a size of 1.5 mm × 1.5 mm, and after electrical connection, they were epoxy-mounted, and the surface was ground using #600 SiC paper and coated with epoxy resin, except for an area of 1 cm^2. The anodic polarization test was performed in sulfuric acid solutions (1, 10, 30, 50, and 70) vol% using a potentiostat (Gamry DC 105). The reference electrode was a saturated calomel electrode (SCE), and the counter electrode was high-density graphite rods. The test solution was de-aerated using nitrogen gas at the rate of 100 mL/min for 30 min and the scanning rate was 0.33 mV/s. The pitting potential, which is the least positive potential at which pits can form was determined from the anodic polarization curve.

2.5 Corrosion product analysis

In order to investigate the corrosion products on the surface after the immersion test in (30 and 70) % H_2SO_4 at 40 ℃, the specimens were cut. The surface and cross-section were observed by SEM (VEGA II LMU, TESCAN) and EPMA (EPMA-1600, Shimadzu). The composition of the corrosion products were observed by Glow Discharge Spectrometry (GDS), (GDS850, LECO).

3. Results

Fig. 1 shows the effect of the concentration of sulfuric acid solution on the corrosion rate of the experimental alloys obtained from the immersion test at 40 ℃ for 3 h. In the case of Ru-bearing alloy AH-2, the corrosion
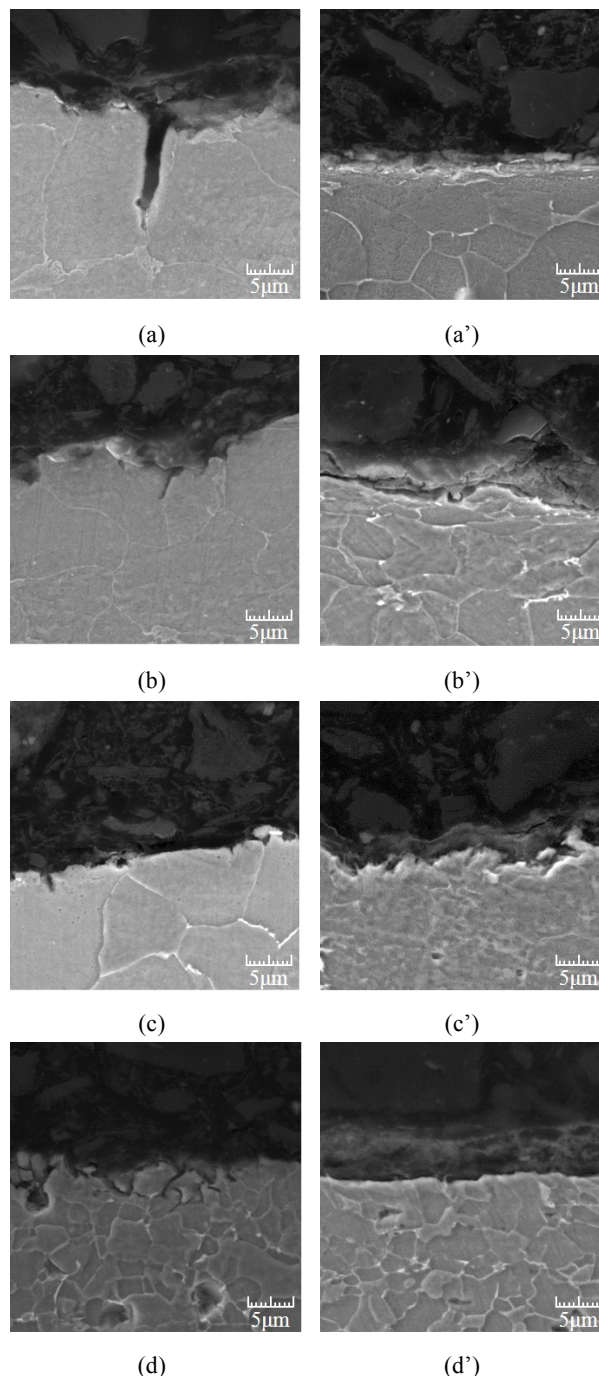

Fig. 2 SEM-images of the cross-section of the experimental alloys after sulfuric acid corrosion test: (a) and (a') AH-1, (b) and (b') AH-2, (c) and (c') AH-3, and (d) and (d') AH-4. (a)-(d): 40 ℃, 30 % H_2SO_4, 3 h immersion test; (a')-(d'): 40 ℃ , 70 % H_2SO_4, 3 h immersion test).

rates were very high at low concentration solutions of (1, 10, and 30) % H_2SO_4. Zn-bearing alloy AH-3 and Ta-bearing alloy AH-4 present a relatively lower corrosion rate than that of the reference alloy AH-1. However, in high
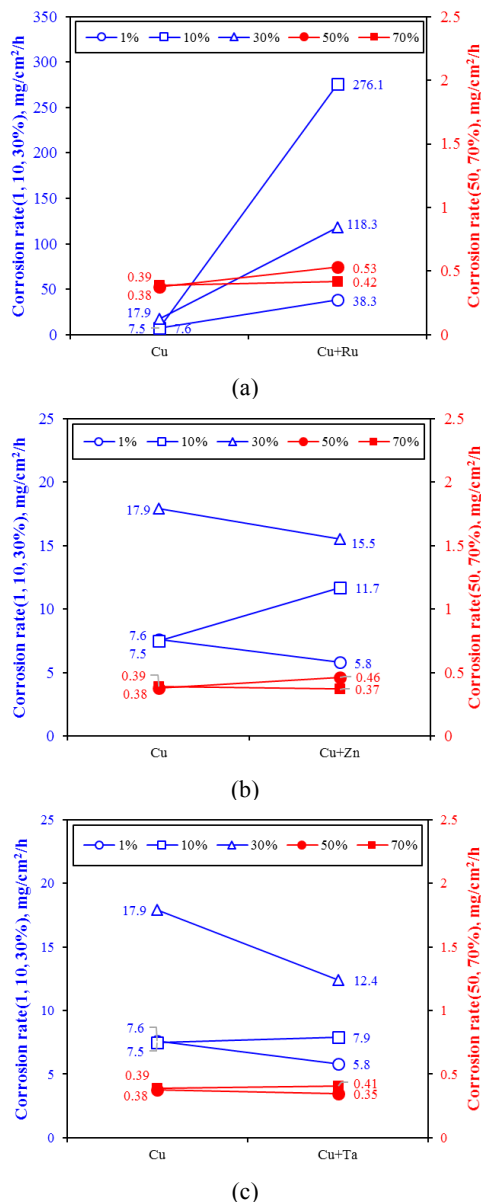
Fig. 3 Effect of alloying elements on the corrosion rate of the experimental alloys (40 °C, 3 h immersion test): (a) Ru addition, (b) Zn addition, and (c) Ta addition, for (1, 10, 30, 50, and 70) % concentration of H₂SO₄.

concentration solutions of 50% and over H₂SO₄, every alloy revealed very low corrosion rates.

In order to find the relation between the corrosion behavior and the concentrations of sulfuric acid, we observed the cross-section of the specimens after the immersion tests. Fig. 2 shows SEM-images of the cross-section of the experimental alloys after the immersion test in (a)-(d) 30% H₂SO₄, and (a')-(d') 70 % H₂SO₄, at 40 °C for 3 h. No protective film formed on the surface of the 4 kinds of specimens tested in 30 % H₂SO₄ solution, and prefer-

ential attacks along the grain boundaries were observed. When the attack was severe, some grains were detached from the matrix. However, increasing the concentration over 50 % H₂SO₄ revealed more different morphologies than those of low concentration under 50 % H₂SO₄. Fig. 2a'-d' show SEM-images of the cross-section of the experimental alloys after sulfuric acid corrosion test in 70 % H₂SO₄ at 40 °C for 3 h. The figures show that the alloys reveal a relatively uniform surface, and a thin layer was observed on the surface. In other words, the alloys in a low concentration of sulfuric acid corroded locally, but the alloys in a high concentration of sulfuric acid formed a thin layer and corroded through this layer.

Fig. 3 represents the effect of alloying elements on the corrosion rate of the experimental alloys; Fig. 3a shows the effect of Ru addition on the corrosion rate in low concentrations (○, □, △) and high concentrations (●, ■) of sulfuric acid solution. Ru addition greatly increased the corrosion rate of low alloy steel, regardless of their concentrations under 30 %. However, in high concentration over 50%, Ru addition only slightly affected the corrosion rate. Fig. 3b shows the effect of Zn addition on the corrosion rate in low concentrations (○, □, △) and high concentrations (●, ■) of sulfuric acid solutions. Zn addition decreased the corrosion rate of low alloy steel except 10 % H₂SO₄ solution in low concentration, but affected the corrosion rate slightly in high concentration over 50 %. Fig. 3c shows the effect of Ta addition on the corrosion rate of low alloy steel in low concentration (○, □, △) and high concentration (●, ■) of sulfuric acid solutions. Ta reduced the corrosion rate of low alloy steel in low concentration of sulfuric acid solutions, but slightly increased the corrosion rate in high concentration over 50 %. That is, in low concentration of sulfuric acid solutions under 30 % H₂SO₄, Zn and Ta additions increased the corrosion resistance of low alloy steel, except for Ru addition. However, Fig. 1 and 3, show that in high concentration solution of sulfuric acid solutions over 50 % H₂SO₄, Ru, Zn, and Ta additions slightly increased the corrosion rate, for both (50 and 70) % H₂SO₄, but their rates were very low.

In order to determine the electrochemical behavior in low and high concentration of sulfuric acid solutions, we performed the anodic polarization tests at 40 °C. The scanning rate was 0.33 mV/sec, and the solutions were deaerated for 30 min. using nitrogen gas at the rate of 200 mL/min. Fig. 4 shows the effect of sulfuric acid concentration on the anodic polarization behavior of the experimental alloys. Regardless of the alloys, anodic current increased by anodic polarization in low concentration of sulfuric acid solution, and passivation didn't occur.
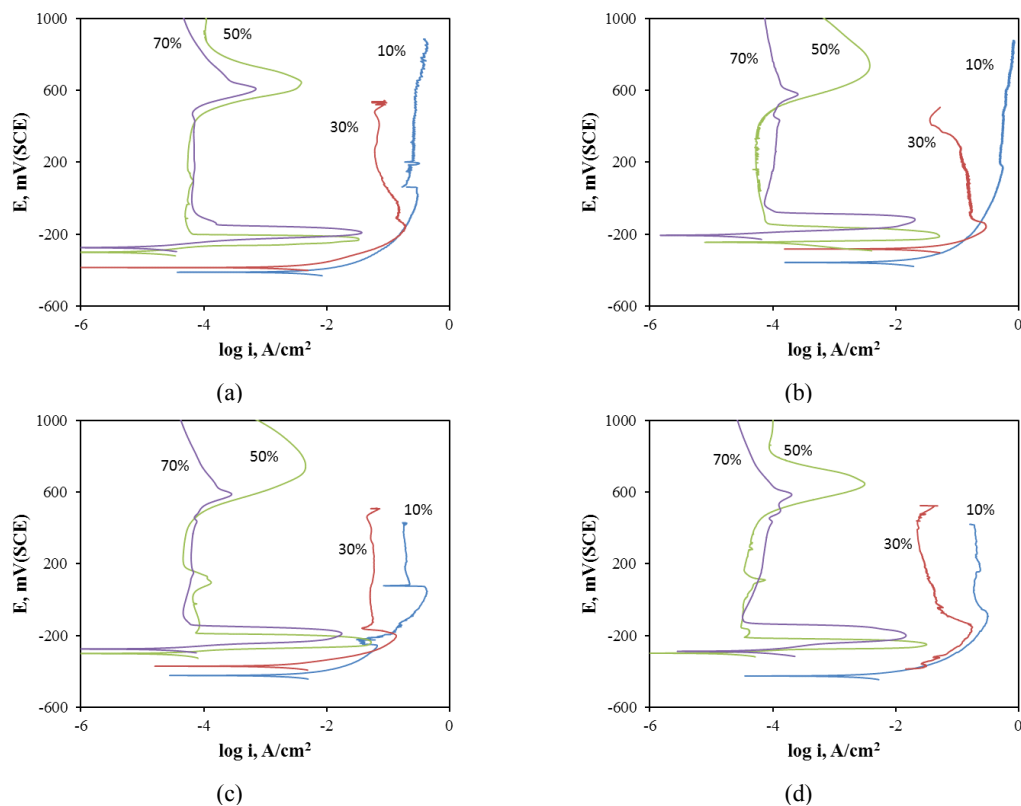
(a)

(b)

(c)

(d)

Fig. 4 Effect of sulfuric acid concentration on the anode polarization behavior of the experimental alloys (40 °C, 0.33 mV/sec): (a) AH-1, (b) AH-2(Ru), (c) AH-3(Zn), and (d) AH-4(Ta), for (1, 10, 30, 50, and 70) % concentration of H₂SO₄.

However, they show excellent passivity by the anodic polarization in high concentration of sulfuric acid solutions. The electrochemical behavior of Fig. 4 is the same as the result of the chemical immersion tests shown in Fig. 1. Therefore, it can be seen that if the concentration of sulfuric acid solution exceeds a critical value, the low alloy steel forms a passive film on the surface and its corrosion rate is abruptly reduced.

4. Discussion

In order to understand whether the electrochemical factors may affect the corrosion rate in sulfuric acid solutions or not, we plotted the Relationship between corrosion rate in H_2SO_4 and electrochemical corrosion factors of the experimental alloys. Anodic current density(i_a) and passive current density(i_p) were determined through anodic polarization curves, and exchange current density(i_0) was determined using a Tafel slope. Fig. 5a-c show the relationship between each factor in the low concentration of 30 % H_2SO_4, while Fig. 5a'-c' show that the relationship between each factor in the high concentration of 70 % H_2SO_4. Fig. 5a and 5a' show that the corrosion rate in low concentration of sulfuric acid was related to the corro-

sion potential, but the rate in the high concentration of sulfuric acid was little related to the corrosion potential. On the other hand, Fig. 5b and 5b' show that the corrosion rate was closely related to the exchange current density (i_0) of H^+/H_2 reaction in the low concentration of sulfuric acid, but the rate in the high concentration of sulfuric acid was only slightly related to the exchange current density. Fig. 5c shows the relationship between the corrosion rate in the low concentration of sulfuric acid and the anodic current density (i_a) at +200 mV(SCE) in Fig. 4. Because the corrosion rate is proportional to the anodic current, it is the natural outcome. Fig. 5c' shows the relationship between the corrosion rate in the high concentration of sulfuric acid and the anodic current density at +200 mV(SCE) in Fig. 4. Fig. 4 shows that the passive films were formed in high concentration of sulfuric acid, regardless of the experimental alloys and the alloys revealed the low passive current density and thus the corrosion rate was abruptly reduced. Therefore, we can summarize that the corrosion rate in a low concentration of sulfuric acid depends upon the exchange current density, but the rate in a high concentration of sulfuric acid depends upon the passive current density.
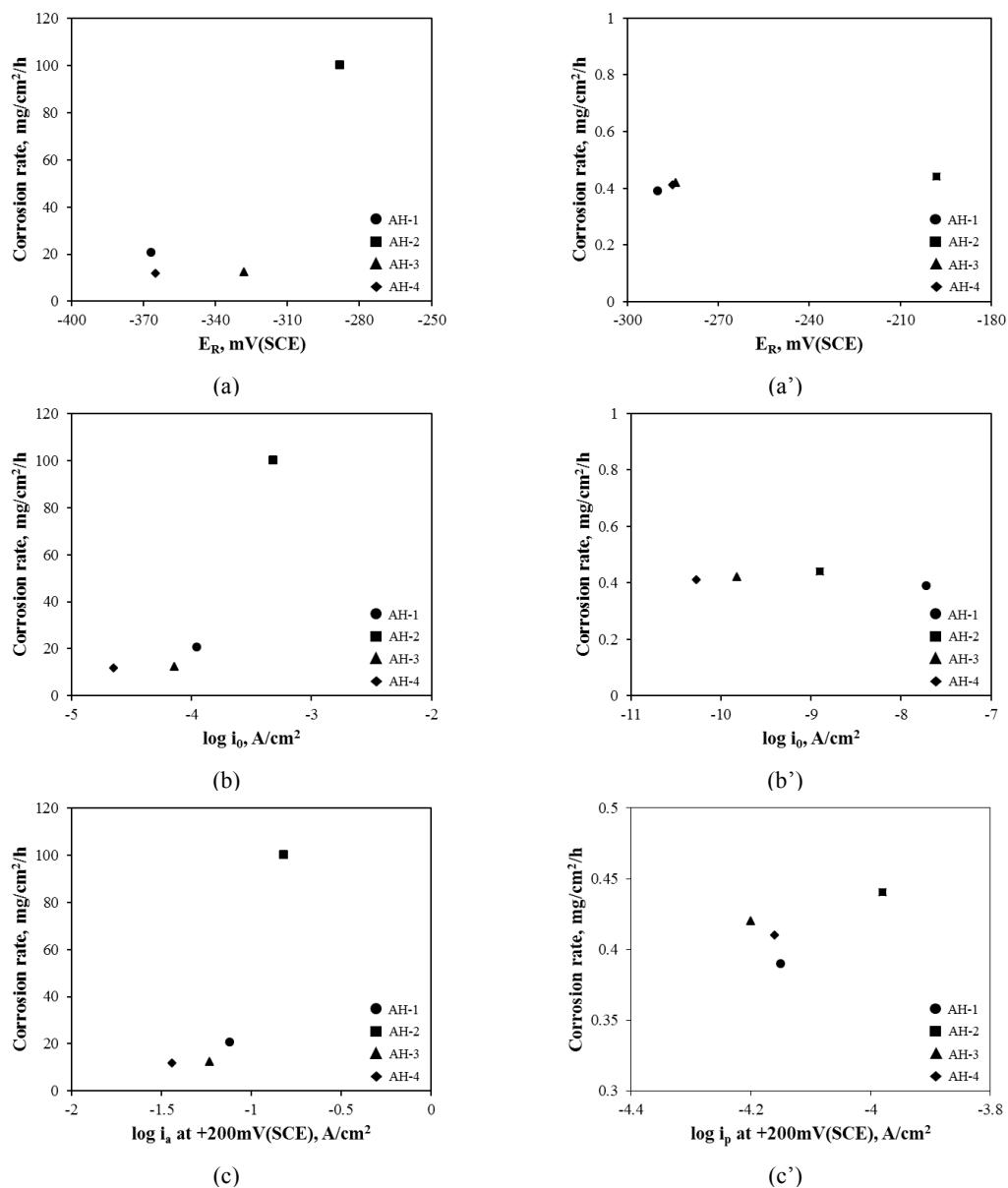
Fig. 5 Relationship between the corrosion rate in H_2SO_4 and the electrochemical corrosion factors of the experimental alloys: (a) and (a') corrosion potential, (b) and (b') exchange current density, and (c) and (c') current density at +200mV(SCE). (a-c): 40 ℃, 30 % H_2SO_4, (a'-c'): 40 ℃, 70 % H_2SO_4).

Fig. 6 was drawn to determine the relationship between the corrosion rate(C-R) by the addition of 3 elements and the electrochemical factors. This figure shows the effect of alloying elements on the corrosion rate and electro-chemical corrosion factors of the experimental alloys. In a low concentration of sulfuric acid, Ru addition increased the exchange current density(i_0) of H^+/H_2 reaction and the anodic current density(i_a) and thus increased the corrosion rate (Fig. 6a). However, in a high concentration of sulfuric acid, Ru addition decreased the exchange current density, but only slightly increased the passive current density(i_p),

and since the corrosion rate was increased by Ru addition, the rate was closely dependent upon the passive current density (Fig. 6a'). In a low concentration of sulfuric acid, Zn addition decreased the exchange current density of H^+/H_2 reaction and the anodic current density, and thus reduced the corrosion rate (Fig. 6b). However, in a high concentration of sulfuric acid, Zn addition decreased the exchange current density, but slightly increased the passive current density, and since the corrosion rate was increased by Zn addition, the rate was closely dependent upon the passive current density (Fig. 6b'). In a low con-
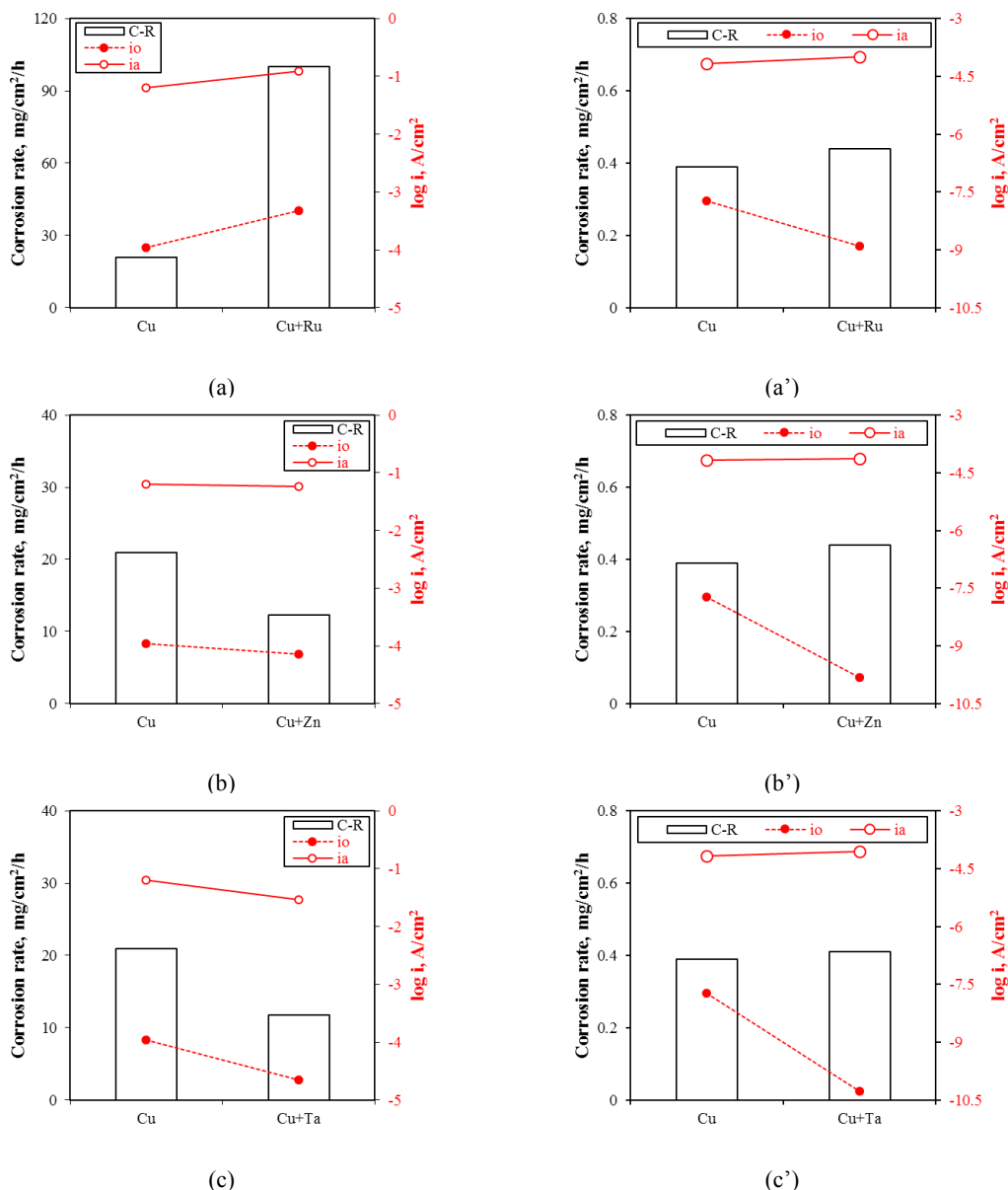
Fig. 6 Effect of alloying elements on corrosion rate and electrochemical corrosion factors of the experimental alloys: (a) and (a') Ru effect, (b) and (b') Zn effect, (c) and (c') Ta effect. (a-c): 40 $^{\circ}$C, 30 % H_2SO_4: (a'-c'): 40 $^{\circ}$C, 70 % H_2SO_4).

centration of sulfuric acid, Ta addition reduced the exchange current density of H^+/H_2 reaction and the anodic current density and thus decreased the corrosion rate (Fig. 6c). However, in a high concentration of sulfuric acid, Ta addition decreased the exchange current density, but slightly increased the passive current density, and since the corrosion rate was increased by Ta addition, the rate was closely depended upon the passive current density. In summary, the alloying element reducing the exchange current density in low concentration of sulfuric acid and the alloying element increasing the passive current density

in high concentration of sulfuric acid, together play an important role in determining the corrosion rate of Cu-bearing low alloy steels.

Fig. 7 reveals the corroded morphologies and elemental distribution by EPMA on the surface of the experimental alloys after the immersion test for 3 h in 30 % H_2SO_4 at 40 $^{\circ}$C. Corroded surfaces were rough and irregular, and these mean the formation of corrosion products on the surface (see Fig. 2). Oxygen was depleted at the Fe-enriched areas and this implies that during the corrosion test, corrosion products may be detached. Cu was enriched at
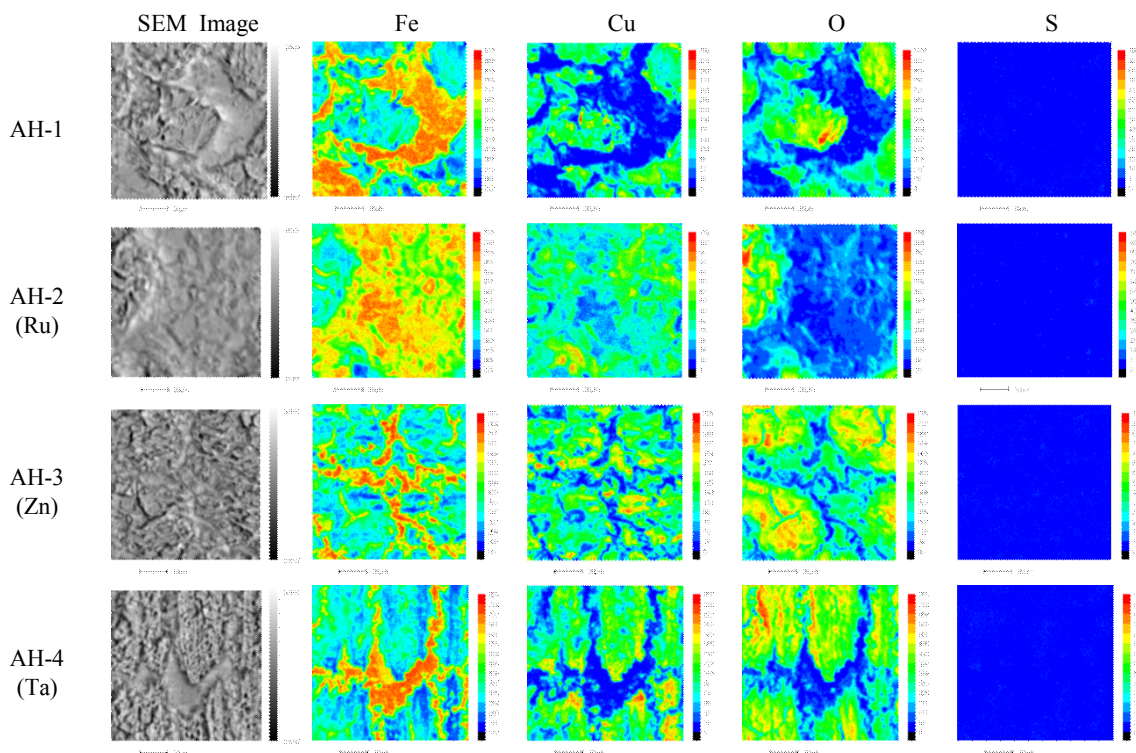
Fig. 7 SEM images and elemental distribution by EPMA on the surface of alloys AH-(1-4) after the corrosion test (40 °C, 30 % H_2SO_4, 3 h immersion test).
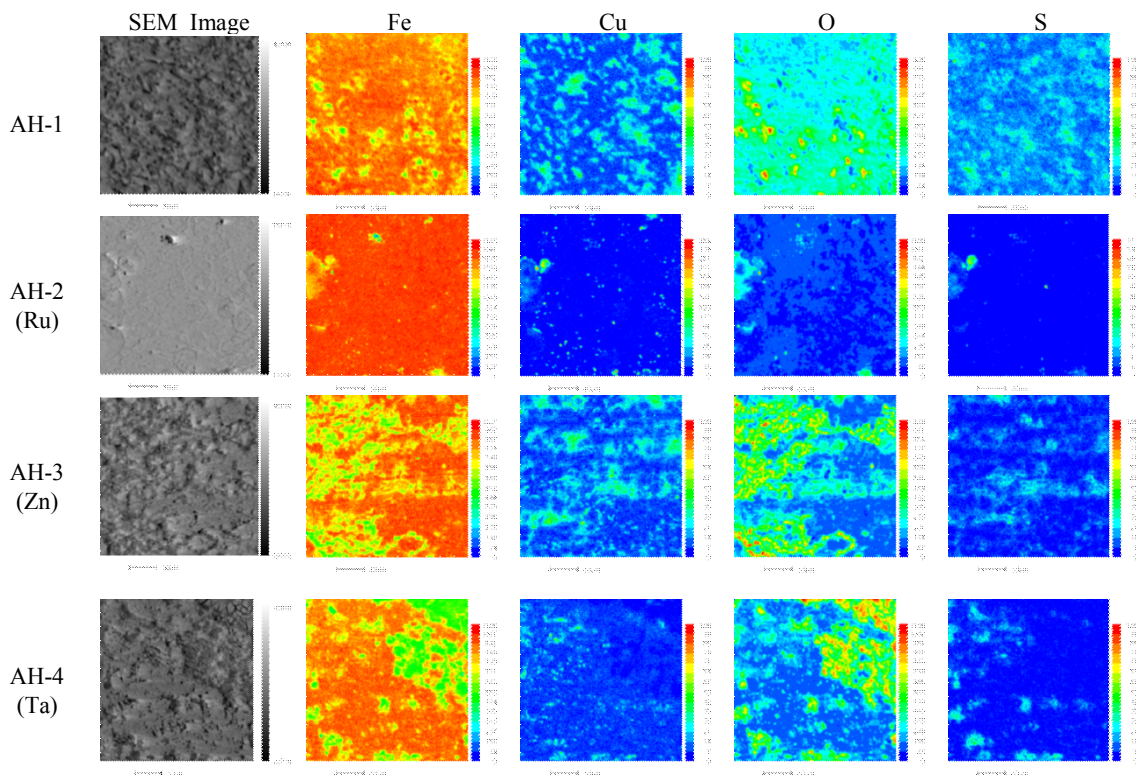

Fig. 8 SEM images and elemental distribution by EPMA on the surface of alloys AH-(1-4) after the corrosion test (40 °C, 70 % H_2SO_4, 3 h immersion test).

(a) Fe

(a') Fe

(b) O
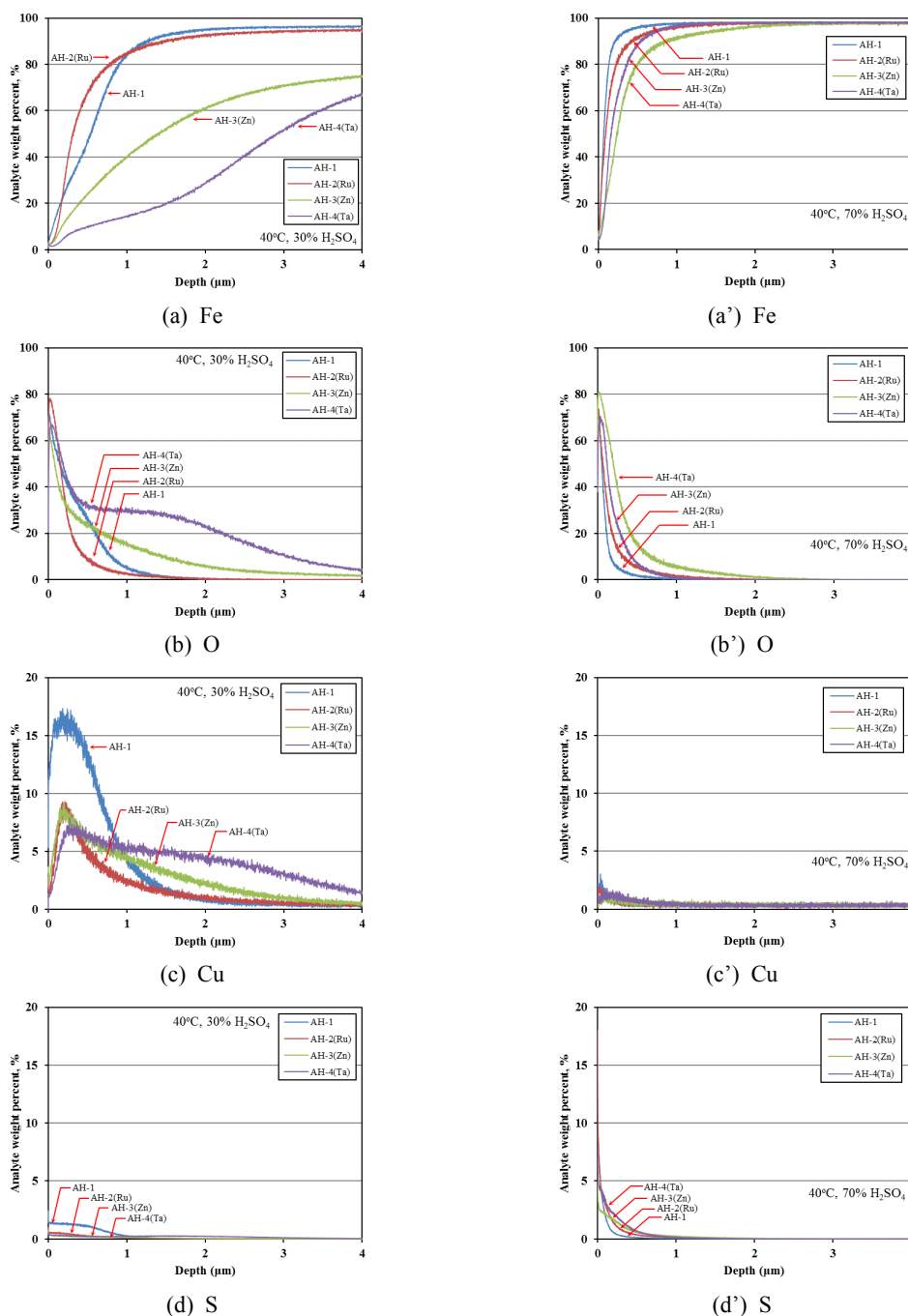

(b') O

(c) Cu

(c') Cu

(d) S

(d') S

Fig. 9 Depth profile by GDS on the surface after the immersion corrosion test for 3 h; (a) and (a') Fe, (b) and (b') O, (c) and (c') Cu, and (d) and (d') S. (a)-(d): 40 °C, 30 % H₂SO₄, (a')-(d'): 40 °C, 70 % H₂SO₄).

the oxygen-enriched areas, but the sulfur wasn't detected at the whole surface. That is, Cu-O enriched areas were partly formed, but some of these products may have detached during the corrosion test. On the other hand, Fig. 8 shows that in high concentration of sulfuric acid, the elements were differently distributed on the surface tested. This figure shows the corroded surface morphologies and

elemental distribution by EPMA on the surface of the experimental alloys after the immersion test for 3 h in 70 % H₂SO₄ at 40 °C. The corroded surface revealed a relative smoothness, and Fe was uniformly distributed, compared with those of the low concentration cases. Oxygen was also relatively uniformly distributed, and Cu and sulfur were locally enriched. That is, it seems that iron oxide

(a) Fe   (a') Fe

(b) O   (b') O

(c) Cu   (c') Cu
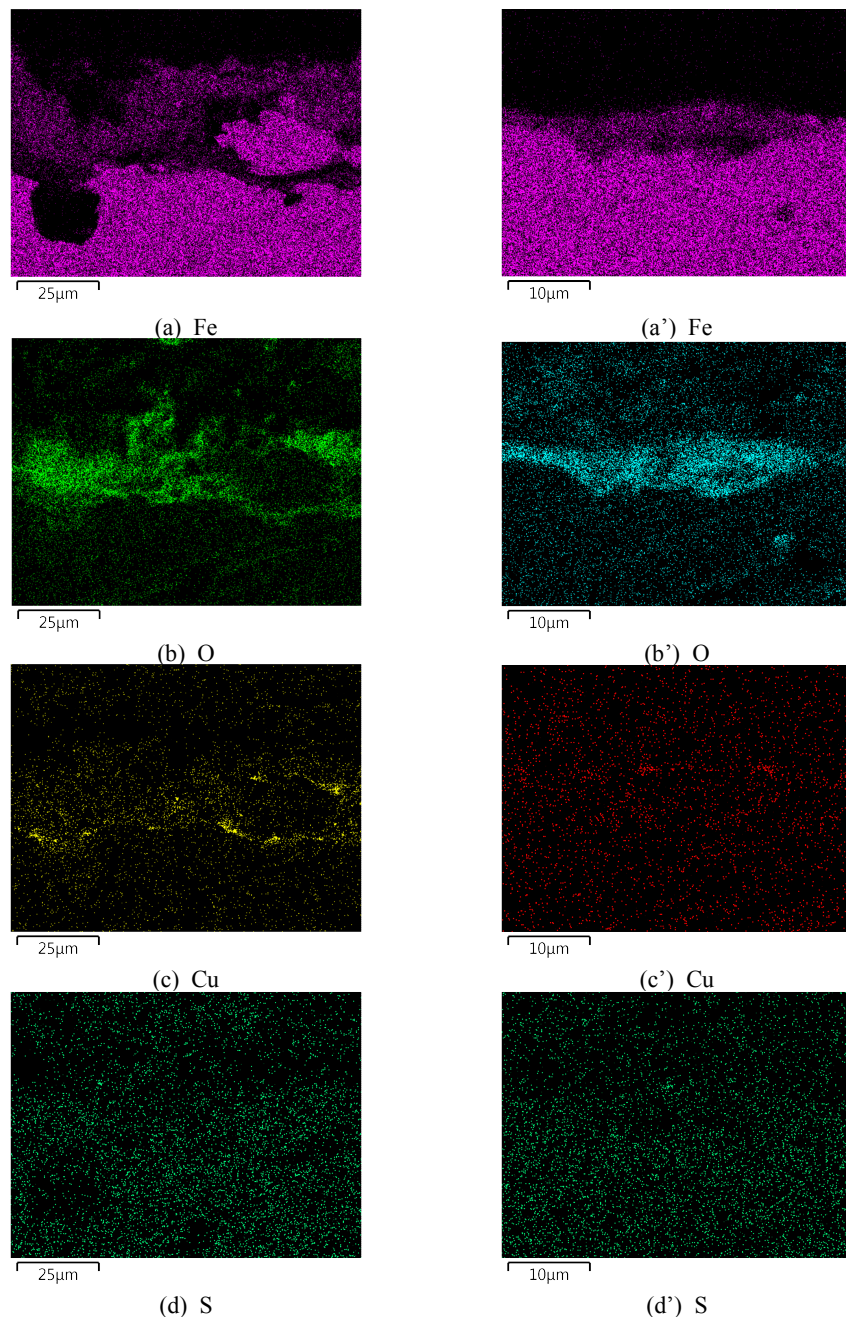
(d) S   (d') S

Fig. 10 Elemental distribution by EPMA on the cross-section of alloy AH-1 after the immersion corrosion test for 3 h; (a) and (a') Fe, (b) and (b') O, (c) and (c') Cu, and (d) and (d') S. (a)-(d): 40 °C, 30 % H$_2$SO$_4$, (a')-(d'): 40 °C, 70 % H$_2$SO$_4$).

layer was formed relatively uniformly and Cu-O-S compounds were locally formed on the surface. Generally, it is well known that Cu could form a protective enriched layer on the surface in acidic solution and increase the corrosion resistance of low alloy steels [6]. However, it is judged that in low concentration of sulfuric acid, Cu-enriched layer can be formed in high concentration of sulfuric acid, but not in low concentration of sulfuric acid.

In order to investigate the composition of the cross-section of the alloys, GDS and EPMA analyses were performed. Fig. 9 shows the depth profile by GDS measurement on the surface after the immersion corrosion test for 3 h in Fig. 9a-d 30 % H$_2$SO$_4$ and Fig. 9a'-d' 70 % H$_2$SO$_4$. In a low concentration of sulfuric acid, Fe and oxygen contents vary greatly with the depth, and it seems that the corrosion product would be thick. As with the
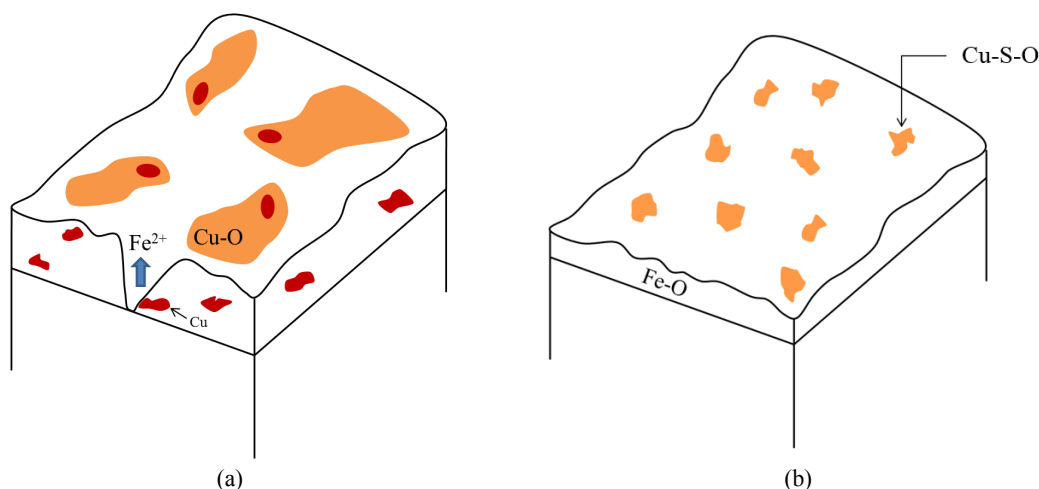
Fig. 11 Effect of the concentration of sulfuric acid on the corrosion mechanism of low alloy steel: (a) low concentration under 30% H₂SO₄, and (b) high concentration over 50% H₂SO₄.

EPMA results in Fig. 7, high levels of Cu contents were detected in depth, but the S contents show very low value. However, in a high concentration of sulfuric acid, a thin layer composed of Fe and oxygen was detected. In the outermost part of the layer, sulfur was enriched with copper. Fig. 10 reveals the elemental distribution by EPMA on the cross-section of alloy AH-1 after the immersion corrosion test for 3 h in Fig. 10a-d 30 % H₂SO₄ and Fig. 10a'-d' 70 % H₂SO₄. In a low concentration of sulfuric acid, it can be seen in Fig. 10a that some grains were detached from the matrix. Fig. 10b shows that thick oxygen layer, and Fig. 10c shows that Cu-enriched areas were detected locally, and it is considered that the detachment of grain from the matrix would be related to the enriched copper area. On the other hand, in a high concentration of sulfuric acid, thin oxide layer was detected, as were Cu-enriched areas, but detachment of grain was not observed.

As described above, it was evaluated that the corrosion rate of Cu-bearing low alloy steel in sulfuric acid depended upon the concentration of sulfuric acid. In low concentration solutions, the corrosion rate was high. Therefore, we proposed the corrosion model with H₂SO₄ concentration as shown in Fig. 11 on the base of the results of the anodic polarization behavior and composition of the surface film; but in high concentration solutions, the rate was very low. For low concentration, this behavior was closely related to the exchange current density and the acceleration of corrosion by the enriched copper areas; and for high concentration, was related to the passive current density and Fe-oxide/Cu-S-O layers, which shown in Fig. 11.

5. Conclusions

In order to elucidate the effects of sulfuric acid concentration and alloying elements on the corrosion properties of Cu-bearing low alloy steel, we performed the chemical and electrochemical tests, and concluded the following:

1) In low concentration of sulfuric acid under 30 % H₂SO₄, the experimental alloys revealed a preferential attack and high corrosion rate, with thick but less dense Cu-O enriched layer formed on the surface, which was confirmed on the cross-section. However, in high concentration of sulfuric acid over 50 %, the alloys showed uniform corrosion and very low corrosion rate, with thin and dense Fe-oxide and Cu-S-O layers formed on the surface, which was confirmed on the cross-section

2) The major factor affecting the corrosion rate of low alloy steels in a low concentration of sulfuric acid solution was the exchange current density for H⁺/H₂ reaction, but the major factors in a high concentration of sulfuric acid solution were with thin and dense passive film, and thereby passivation behavior.

3) The alloying elements reducing the exchange current density in low concentration of sulfuric acid, and the alloying elements decreasing the passive current density in high concentration of sulfuric acid, together play an important role in determining the corrosion rate of Cu-bearing low alloy steels in a wide range of sulfuric acid solution.

Acknowledgement

References

1. A. K. Sharma, D. S. N. Prasad, S. Acharya, and R. Sharma, *Int. J. Chem. Eng. Appl.*, **3**, 129 (2012).
2. J. T. Lee and M. C. Chen, *Using Seawater to Remove SO₂ in a FGD System*, open access, p. 427, Waste Water - Treatment and Reutilization, InTech, London (2011).
3. J. E. Staudt, S. R. Khan, and M. J. Oliva, *Proc. Combined Power Plant Air Pollutant Control Mega Symposium 2004*, Paper # 04-A-56-AWMA, Washington (2004).
4. D. Kelley, *J. Reinf. Plast. Comp.,* **51**, 14, (2007).
5. S. A. Park and J. G. Kim, *Kor. J. Met. Mater.*, **52**, 837 (2014).
6. M. Seo, G. Hultquist, C. Leygraf, and N. Sato, *Corros. Sci.*, **26**, 949 (1986).
7. A. Yamamoto, T. Ashiura, and E. Kamisaka, *Corros. Eng.*, **35**, 48, (1986).
8. J. Okamoto, A. Usami, and H. Mimura, *Nippon Steel Technical Report*, **87**, 46 (2003).
9. J. Y. Park, K. J. Chung, and S. H. Lee, *POSCO Research paper*, **12**, 23 (2007).
10. S. H. Kim, S. A. Park, J. G. Kim, K. S. Shin, and Y. He, *Met. Mater. Int.*, **21**, 232 (2015).
11. A. Pardo, M. C. Merino, *Corros. Sci.*, **48**, 1075 (2006).
12. K. N. Oh, and S. H Ahn, *Electrochim. Acta*, **88**, 170 (2013).
13. J. H. Hong, S. H. Lee, and J. G. Kim, *Corros. Sci.*, **54**, 174 (2012).
14. J. S. Lee, S. T. Kim, and I. S. Lee, *Mater. Trans.*, **53**, 1048 (2012).
15. S. T. Kim, Y. S. Park, H. J. Kim, *Corros. Sci. Tech.*, **28**, 281 (1999).
16. H. E. Townsend, *Corrosion*, **57**, 497 (2001).
17. H. E. Townsend, T. C. Simpson, and G. L. Jhonson, *Corrosion*, **50**, 546 (1994).
18. M. J. Kim and J. G. Kim, *Int. J. Electrochem. Sci.,* **10**, 6872 (2015).
19. K. H. Kim, S. H. Lee, N. D. Nam, and J. G. Kim, *Corros. Sci.*, **53**, 3576 (2011).
20. S. A. Park, J. G. Kim, and J. B. Yoon, *Corrosion*, **70**, 196 (2014).
21. D. Devilliers, M. T. Dinh, E. Mahe, D. Krulic, N. Larabi and N. Fatouros, *J. New. Mat, Electrochem. systems*, **2**, 221 (2006).
22. N. D. Nam and J. G. Kim, *Corros. Sci.*, **52**, 3337 (2010).
23. L. L. Wikstrom, N. T. Thomas, and K. Nobe, *J. Electrochem. Soc.*, **122**, 1201 (1975).
24. M. Metikos-Hukovic and B. Lovrecek, *Electrochim. Acta*, **25**, 717 (1979).
25. IARC, Antimony trioxide and antimony trisulfide, *IARCMonog. Eval. Carc*, **47**, 291 (1989).
26. NARS, Main Issues regarding the Introduction of the Good Samaritan Law, **90**, 67, (2010).
27. S. Uttiya, D. Contarino, S. Prandi, M. Carnasciali, G. Gemme, L. Mattera, R. Rolandi, M. Canepa, and O. Cavalleri, *J. Mater. Sci. Nanotechnol.*, **1**, 1 (2014).
28. A. S. Mogoda, W. A. Badawy and M. M. Ibrahim, *Indian J. Chem. Techn.*, **2**, 217 (1995).
29. D. L. Graver, *Corrosion data survey-Metals section*, 6th ed., p. 69, NACE, Texas (1985).
30. J. H. Potgieter, W. Skinner, and A. M. Heyns, *INCSAC*, **2**, 235 (1992).
31. P. P. Sharma and I. I. Suni, *J. Electrochem. Soc.*, **158**, H111 (2011).
32. E. B. Ituen, *Advan. Appl. Sci. Res.*, **5**, 26 (2014).
33. S. A. Odoemelam, E. C. Ogoko, B. I. Ita, N. O. Eddy, *Port. Electrochim. Acta*, **27**, 57 (2009).